NASA/TM–2019–220285

Bowles-TatnallWake Vortex Encounter Hazard Metric

Joel Malissa
University of Pennsylvania, Philadelphia, Pennsylvania

Nashat N. Ahmad
Langley Research Center, Hampton, Virginia

June 2019

NASA STI Program...in Profile

Since its founding, NASA has been dedicated to the advancement of aeronautics and space science. The NASA scientific and technical information (STI) program plays a key part in helping NASA maintain this important role.

The NASA STI Program operates under the auspices of the Agency Chief Information Officer. It collects, organizes, provides for archiving, and disseminates NASA's STI. The NASA STI Program provides access to the NASA Aeronautics and Space Database and its public interface, the NASA Technical Report Server, thus providing one of the largest collection of aeronautical and space science STI in the world. Results are published in both non-NASA channels and by NASA in the NASA STI Report Series, which includes the following report types:

- TECHNICAL PUBLICATION. Reports of completed research or a major significant phase of research that present the results of NASA programs and include extensive data or theoretical analysis. Includes compilations of significant scientific and technical data and information deemed to be of continuing reference value. NASA counterpart of peer-reviewed formal professional papers, but having less stringent limitations on manuscript length and extent of graphic presentations.

- TECHNICAL MEMORANDUM. Scientific and technical findings that are preliminary or of specialized interest, e.g., quick release reports, working papers, and bibliographies that contain minimal annotation. Does not contain extensive analysis.

- CONTRACTOR REPORT. Scientific and technical findings by NASA-sponsored contractors and grantees.

- CONFERENCE PUBLICATION. Collected papers from scientific and technical conferences, symposia, seminars, or other meetings sponsored or co-sponsored by NASA.

- SPECIAL PUBLICATION. Scientific, technical, or historical information from NASA programs, projects, and missions, often concerned with subjects having substantial public interest.

- TECHNICAL TRANSLATION. English-language translations of foreign scientific and technical material pertinent to NASA's mission.

Specialized services also include organizing and publishing research results, distributing specialized research announcements and feeds, providing information desk and personal search support, and enabling data exchange services.

For more information about the NASA STI Program, see the following:

- Access the NASA STI program home page at `http://www.sti.nasa.gov`

- E-mail your question to `help@sti.nasa.gov`

- Phone the NASA STI Information Desk at 757-864-9658

- Write to:
  NASA STI Information Desk
  Mail Stop 148
  NASA Langley Research Center
  Hampton, VA 23681-2199

NASA/TM–2019–220285

Bowles-TatnallWake Vortex Encounter Hazard Metric

Joel Malissa
University of Pennsylvania, Philadelphia, Pennsylvania

Nashat N. Ahmad
Langley Research Center, Hampton, Virginia

National Aeronautics and
Space Administration

Langley Research Center
Hampton, Virginia 23681-2199

June 2019

Available from:

NASA STI Program / Mail Stop 148
NASA Langley Research Center
Hampton, VA 23681-2199
Fax: 757-864-6500

Contents

Nomenclature

Γ_0	Initial vortex circulation (m^2/s)
λ_F	Following aircraft wing taper ratio
Φ	Bank angle of the following aircraft (rad)
$(AR)_G$	Aspect ratio of the generating aircraft wing
b_F	Following aircraft wing span (m)
b_G	Generating aircraft wing span (m)
c_F	Following aircraft wing chord (m)
$C_{L\alpha F}$	Three-dimensional lift-curve slope of following aircraft (rad^{-1})
C_{LG}	Lift coefficient of the generating aircraft
C_{lv}	Vortex-induced rolling moment coefficient
C_{Lv}	Vortex-induced lift coefficient
$\bar{q}$	Freestream dynamic pressure (kg/m^2)
r_c	Vortex-core radius (m)
s	Half of the vortex pair separation distance (m)
S_F	Following aircraft wings planform area (m^2)
V_F	Velocity of the following aircraft (m/s)
V_G	Generating aircraft velocity (m/s)
Y	Inertial lateral coordinate (m)
Y_F	Lateral location of the following aircraft (m)
Z	Inertial vertical coordinate (m)
Z_F	Vertical location of the following aircraft (m)

1. Introduction

Wake vortex spacing standards constrict the terminal area throughput and impose severe constraints on the overall capacity and efficiency of the National Airspace System. For more than two decades starting in the early 1990s, the National Aeronautics and Space Administration conducted extensive research on characterizing the formation and evolution of aircraft wakes. This multidisciplinary work included comprehensive field experiments (Pruis et al. 2016), flight tests (Vicroy et al. 1998), and wind tunnel tests (Rossow 1994; Chow et al. 1997). Parametric studies using large eddy simulations (Proctor 1998; Proctor et al. 2006) were conducted in order to develop fast-time models for the prediction of wake transport and decay (Ahmad et al. 2016). Substantial effort was spent on the formulation of acceptable vortex hazard metrics (Tatnall 1995; Hinton and Tatnall 1997).

Several wake encounter severity metrics have been suggested in the past, which include the wake circulation strength, vortex-induced rolling moment coefficient (C_{lv}), bank angle, and the roll control ratio (Tatnall 1995; Hinton and Tatnall 1997; Van der Geest 2012). The vortex-induced rolling moment coefficient introduced by Bowles and Tatnall (Tatnall 1995; Gloudemans et al. 2016) has been used extensively for risk and safety analysis of newly proposed air traffic management concepts and procedures. The original method of Bowles and Tatnall assumed a constant wing loading (the wing lift-curve slope, $C_{L\alpha}$ is constant), which resulted in an overestimation of the vortex-induced rolling moment coefficient. Bowles (2014) suggested a correction to the original method that provides more accurate values of C_{lv} and which is also consistent with the underlying physics of the problem. The overestimation of C_{lv} in the original method can be corrected by assuming an elliptical lift distribution. Figure 1.1 illustrates the correction in C_{lv} achieved by the modified method.

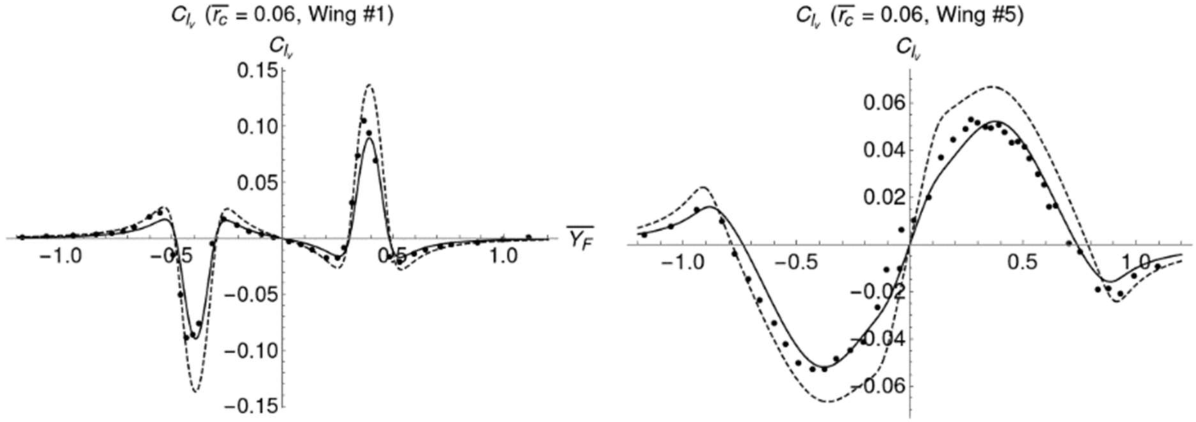

Figure 1.1: Comparison of the vortex-induced rolling moment coefficient using constant and elliptical wing loadings with the wind tunnel data (Rossow 1994). Dashed line denotes a constant wing loading and solid line denotes an elliptical wing loading. The wind tunnel data are given by points in the plots. Results are shown for two different wings used in the wind tunnel test.

The assumption of constant wing loading in their original formulation had allowed Bowles and Tatnall to derive a closed-form analytical solution, which was computationally efficient and convenient to use. The addition of elliptical loading term added complexity that required numerical integration. This brief note presents a closed-form analytical solution to the modified Bowles-Tatnall method. The analytical solutions for both the vortex-induced rolling moment coefficient and the vortex-induced lift are compared with results obtained using numerical integration. The resulting analytical method is robust, computationally efficient (more than ten times faster compared to numerical integration), and convenient to use. The simplicity of the method will allow efficient calculations of large leader-follower aircraft matrices in the safety analyses of new procedures. It can also be used on the flight deck for future operations such as dynamic self-separation of aircraft.

2. Vortex-Induced Rolling Moment and Lift Coefficients

The derivation of the analytical expression for the vortex-induced rolling moment and lift coefficients is given in this section. The axis conventions follow Tatnall (1995) and are shown in Figure 2.1.

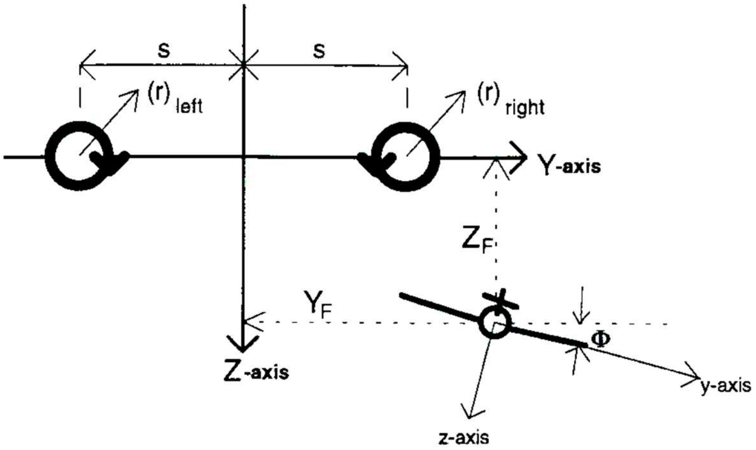

Figure 2.1. Axis conventions and nomenclature as defined by Tatnall (1995).

The Bowles-Tatnall vortex-induced rolling moment coefficient (Tatnall 1995) is given by:

$$C_{lv} = \frac{2C_{L_G} C_{L_{\alpha F}} V_G b_G^2}{\pi^2 (AR)_G b_F^2 (1+\lambda_F) V_F} \int_{-b_F/2b_G}^{b_F/2b_G} \left\{ \begin{array}{l} \bar{y}\left(1 - \dfrac{2b_G(1-\lambda_F)}{b_F}\left|\bar{y}\right|\right) \bullet \\ \left[\left(\dfrac{\bar{y} + (\bar{Y}_F + \bar{s})\cos(\Phi) + \bar{Z}_F \sin(\Phi)}{\bar{y}^2 + \bar{y}\left(2(\bar{Y}_F + \bar{s})\cos(\Phi) + 2\bar{Z}_F \sin(\Phi)\right) + \left((\bar{Y}_F + \bar{s})^2 + \bar{Z}_F^2 + \bar{r}_c^2\right)}\right) \right. \\ \left. - \left(\dfrac{\bar{y} + (\bar{Y}_F - \bar{s})\cos(\Phi) + \bar{Z}_F \sin(\Phi)}{\bar{y}^2 + \bar{y}\left(2(\bar{Y}_F - \bar{s})\cos(\Phi) + 2\bar{Z}_F \sin(\Phi)\right) + \left((\bar{Y}_F - \bar{s})^2 + \bar{Z}_F^2 + \bar{r}_c^2\right)}\right)\right] \end{array} \right\} d\bar{y}\ , \tag{2.1}$$

where, C_{L_G} is the lift coefficient of the vortex generator, $C_{L_{\alpha F}}$ is the three-dimensional lift-curve slope of the follower, V_F and V_G are the airspeeds of the follower and the vortex generator, respectively, b_F and b_G are the wingspans of the follower and generator, respectively. $(AR)_G$ is the wing aspect ratio of the generator, λ_F is the wing taper ratio of the follower, s is the half of vortex pair separation, r_c is the vortex core radius size, Φ is the bank angle of the follower, and (Y_F, Z_F) is the follower's center of gravity in inertial coordinates. The overbar symbol implies normalization by the generator wingspan, b_G.

Eq. (2.1) can be rewritten by substituting

$$\Gamma_0 = \frac{2C_{L_G} b_G V_G}{\pi (AR)_G}\ , \tag{2.2}$$

where, Γ_0 is the circulation strength of the generator's wake vortex,

$$C_{lv} = \frac{\Gamma_0 C_{L_{\alpha F}} b_G}{\pi b_F{}^2 \left(1+\lambda_F\right) V_F} \int\limits_{-b_F/2b_G}^{b_F/2b_G} \left\{ \begin{gathered} \bar{y}\left(1 - \frac{2b_G\left(1-\lambda_F\right)}{b_F}\left|\bar{y}\right|\right) \bullet \\ \left[\left(\frac{\bar{y} + \left(\bar{Y}_F + \bar{s}\right)\cos(\Phi) + \bar{Z}_F \sin(\Phi)}{\bar{y}^2 + \bar{y}\left(2\left(\bar{Y}_F + \bar{s}\right)\cos(\Phi) + 2\bar{Z}_F \sin(\Phi)\right) + \left(\left(\bar{Y}_F + \bar{s}\right)^2 + \bar{Z}_F^2 + \bar{r}_c^2\right)} \right) \right. \\ \left. - \left(\frac{\bar{y} + \left(\bar{Y}_F - \bar{s}\right)\cos(\Phi) + \bar{Z}_F \sin(\Phi)}{\bar{y}^2 + \bar{y}\left(2\left(\bar{Y}_F - \bar{s}\right)\cos(\Phi) + 2\bar{Z}_F \sin(\Phi)\right) + \left(\left(\bar{Y}_F - \bar{s}\right)^2 + \bar{Z}_F^2 + \bar{r}_c^2\right)} \right) \right] \end{gathered} \right\} d\bar{y} \, . \tag{2.3}$$

The integrals in Eq. (2.1) and (2.3) assume a constant lift distribution across the wingspan, which simplifies the integral and allows closed-form solution for the rolling moment coefficient:

$$C_{lv} = K_{lv}\left(I_1 - I_2\right), \tag{2.4}$$

where,

$$K_{lv} = \left(\frac{\Gamma_0}{\pi}\right)\left(\frac{C_{L_\alpha F} b_G}{b_F^2 V_F}\right)\left(\frac{1}{1+\lambda_F}\right). \tag{2.5}$$

I_1 and I_2 are defined as follows:

$$\begin{gathered} I_i = \frac{1}{2}\left[\left(C_i^2 - A_i^2\right)\Omega - C_i\right]\ln\left[\frac{C_i^2 + A_i^2}{\left(C_i - B\right)^2 + A_i^2}\right] + \frac{1}{2}\left[\left(C_i^2 - A_i^2\right)\Omega + C_i\right]\ln\left[\frac{C_i^2 + A_i^2}{\left(C_i + B\right)^2 + A_i^2}\right] + \\ A_i\left[4C_i\Omega\tan^{-1}\left(\frac{C_i}{A_i}\right) + \left(1 - 2C_i\Omega\right)\tan^{-1}\left(\frac{C_i - B}{A_i}\right) - \left(1 + 2C_i\Omega\right)\tan^{-1}\left(\frac{C_i + B}{A_i}\right)\right] \qquad i = 1,2 \end{gathered} \, . \tag{2.6}$$

The parameters, C_1, C_2, A_1, A_2, B, and Ω in Eq. (2.6) are given by

$$C_1 = \left(\bar{Y}_F + \bar{s}\right)\cos(\Phi) + \bar{Z}_F \sin(\Phi), \tag{2.7}$$

$$C_2 = \left(\bar{Y}_F - \bar{s}\right)\cos(\Phi) + \bar{Z}_F \sin(\Phi), \tag{2.8}$$

$$A_1^2 = \left[\left(\bar{Y}_F + \bar{s}\right)\sin(\Phi) - \bar{Z}_F \cos(\Phi)\right]^2 + \bar{r}_c^2, \tag{2.9}$$

$$A_2^2 = \left[\left(\bar{Y}_F - \bar{s}\right)\sin(\Phi) - \bar{Z}_F \cos(\Phi)\right]^2 + \bar{r}_c^2, \tag{2.10}$$

$$B = \frac{b_F}{2b_G}, \tag{2.11}$$

$$\Omega = \frac{1 - \lambda_F}{B}. \tag{2.12}$$

The overbar symbol implies normalization by the generator wingspan, b_G, e.g., $\bar{Z}_F = \frac{Z_F}{b_G}$.

The modification to Eq. (2.3) with elliptical wing loading proposed by Bowles is given in Eq. (2.13). This addition complicated the integral by introducing a square root term and until now required numerical integration for its solution,

$$C_{lw} = K_{lw} \int_{-B}^{B} \left[\overline{y}(1 - \Omega|\overline{y}|) \sqrt{1 - \left(\frac{\overline{y}}{B} \right)^2} \left(\frac{\overline{y} + C_1}{(\overline{y} + C_1)^2 + A_1^2} - \frac{\overline{y} + C_2}{(\overline{y} + C_2)^2 + A_2^2} \right) \right] d\overline{y} \, . \tag{2.13}$$

The analytical solution of Eq. (2.13) can be found by first separating the integral given in Eq. (2.13) according to

$$\int_{-a}^{a} f\left(|x|\right) dx = \int_{-a}^{0} f\left(-x\right) dx + \int_{0}^{a} f\left(x\right) dx, \;\; if \;\; a > 0 \, . \tag{2.14}$$

The resulting integrands are factored into terms of the form $\frac{p_1\left(x\right)\sqrt{p_2\left(x\right)}}{p_2\left(x\right)}$, where $p_n\left(x\right)$ is a polynomial of degree *n*. Applying rule-based integration (Rich et al. 2018) leads to an analytical solution. These rules are described below:

If $e^2 - 4df \neq 0$, $p = \frac{1}{2}$, and $q = -1$, then

$$\begin{aligned} &\int \left(g + hx\right)\left(a + cx^2\right)^p \left(d + ex + fx^2\right)^q dx \\ &= \frac{h\left(a + cx^2\right)^p}{2fp} \\ &+ \frac{1}{2fp} \int \left(a + cx^2\right)^{p-1} \left(d + ex + fx^2\right)^q \left(ahep - ap(he - 2gf) - 2hp(cd - af)x - (hcep + cp(he - 2gf))x^2\right) dx. \end{aligned} \tag{2.15}$$

If $n = 2$, and $p = \frac{1}{2}$, then

$$\int \left(a + bx^n\right)^p dx = \frac{x\left(a + bx^n\right)^p}{np + 1} + \frac{anp}{np + 1} \int \left(a + bx^n\right)^{p-1} dx \, . \tag{2.16}$$

If $b^2 - 4ac \neq 0$, then

$$\int \frac{A + Bx + Cx^2}{(a + bx + cx^2)\sqrt{d + fx^2}} dx = \frac{C}{c} \int \frac{1}{\sqrt{d + fx^2}} dx + \frac{1}{c} \int \frac{Ac - aC + (Bc - bC)x}{(a + bx + cx^2)\sqrt{d + fx^2}} dx \, . \tag{2.17}$$

Let $q = \sqrt{\left(cd - af\right)^2 + b^2 df}$, and if $b^2 - 4ac < 0$, then

$$\begin{aligned} &\int \frac{g + hx}{(a + bx + cx^2)\sqrt{d + fx^2}} dx \\ &= \frac{1}{2q} \int \frac{hbd - g(cd - af - q) + (h(cd - af + q) + gbf)x}{(a + bx + cx^2)\sqrt{d + fx^2}} dx \\ &- \frac{1}{2q} \int \frac{hbd - g(cd - af + q) + (h(cd - af - q) + gbf)x}{(a + bx + cx^2)\sqrt{d + fx^2}} dx. \end{aligned} \tag{2.18}$$

Let $u = \frac{gb - 2ah - (bh - 2gc)x}{\sqrt{d + fx^2}}$, and if $b^2 - 4ac \neq 0$, and $bh^2 d - 2gh\left(cd - af\right) - g^2 bf = 0$, then

$$\int \frac{g + hx}{\left(a + bx + cx^2\right)\sqrt{d + fx^2}} dx = -2g\left(gb - 2ah\right) \int \frac{1}{g\left(gb - 2ah\right)\left(b^2 - 4ac\right) - bdu^2} du \, . \tag{2.19}$$

If $a > 0$, and $b < 0$, then

$$\int \frac{1}{\sqrt{a + bx^2}}\,dx = \frac{\sin^{-1}\left(\dfrac{\sqrt{-b}x}{\sqrt{a}}\right)}{\sqrt{-b}}. \tag{2.20}$$

If $\frac{a}{b} > 0$, then

$$\int \frac{1}{a + bx^2}\,dx = \frac{\sqrt{\dfrac{a}{b}}\tan^{-1}\left(\dfrac{x}{\sqrt{a / b}}\right)}{a}. \tag{2.21}$$

If $\frac{a}{b} < 0$, then

$$\int \frac{1}{a + bx^2}\,dx = \frac{\sqrt{-\dfrac{a}{b}}\tanh^{-1}\left(\dfrac{x}{\sqrt{-a / b}}\right)}{a}. \tag{2.22}$$

After applying these rules in Mathematica® and simplifying, the vortex-induced rolling moment coefficient can be written as,

$$C_{lv} = \frac{K_{lv}}{2B}\sum_{j=1}^{4}\left\{\left(-1\right)^j I_j\left[\left(\pi - 2B\Omega\right)I_j + \sqrt{B^2 + I_j^2}\left(2\Omega\tanh^{-1}\left(\frac{B}{\sqrt{B^2 + I_j^2}}\right)I_j - \pi\right)\right]\right\}, \tag{2.23}$$

where,

$$I_j = \sqrt{\left[\left(\overline{Y}_F - (-1)^j\overline{s}\right)\sin(\Phi) - \overline{Z}_F\cos(\Phi)\right]^2 + \overline{r}_c^{\,2}} + i\left[\cos\left(\frac{j\pi}{2}\right) + \sin\left(\frac{j\pi}{2}\right)\right]\left[\left(\overline{Y}_F - (-1)^j\overline{s}\right)\cos(\Phi) + \overline{Z}_F\sin(\Phi)\right]. \tag{2.24}$$

Complex numbers have been used to condense Eq. (2.23)-(2.24). An equivalent but less elegant form with only real terms can be obtained by using the conversion formulae, e.g.,

$$\tanh^{-1}\left(z\right) = \frac{1}{2}\left[\ln\left(1 + z\right) - \ln\left(1 - z\right)\right],\ \ln\left(z\right) = \ln\left(r\right) + i\theta, \text{ and } z = x + iy = re^{i\theta} = r\left(\cos\left(\theta\right) + i\sin\left(\theta\right)\right).$$

The modified vortex-induced lift coefficient with elliptical loading is given by,

$$C_{Lv} = K_{Lv}\int_{-B}^{B}\left[(1 - \Omega\left|\overline{y}\right|)\sqrt{1 - \left(\frac{\overline{y}}{B}\right)^2}\left(\frac{\overline{y} + C_1}{(\overline{y} + C_1)^2 + A_1^2} - \frac{\overline{y} + C_2}{(\overline{y} + C_2)^2 + A_2^2}\right)\right]d\overline{y}. \tag{2.25}$$

An analytical expression can be found for the lift coefficient by using the same substitution rules described earlier in Eq. (2.14)-(2.22),

$$C_{Lv} = \\ \frac{K_{Lv}}{2B}\left\{4(\pi - 2B\Omega)\overline{s}\cos(\Phi) + i\sum_{j=1}^{4}\left[\left(\cos\left(\frac{(j+1)\pi}{2}\right) + \sin\left(\frac{(j+1)\pi}{2}\right)\right)\sqrt{B^2 + I_j^2}\cdot\left(2\Omega\tanh^{-1}\left(\frac{B}{\sqrt{B^2 + I_j^2}}\right)I_j - \pi\right)\right]\right\} \tag{2.26}$$

where, I_j is defined as in Eq. (2.24), and K_{Lv} is given by:

$$K_{Lv} = -\frac{2C_{L_G} C_{L\alpha F} V_G}{\pi^2 \left(AR\right)_G \left(b_F / b_G\right)\left(1+\lambda_F\right) V_F} . \tag{2.27}$$

Figures 2.2 and 2.3 show the comparison of analytical method with the results obtained using numerical integration for the vortex-induced rolling moment and lift coefficients, respectively.

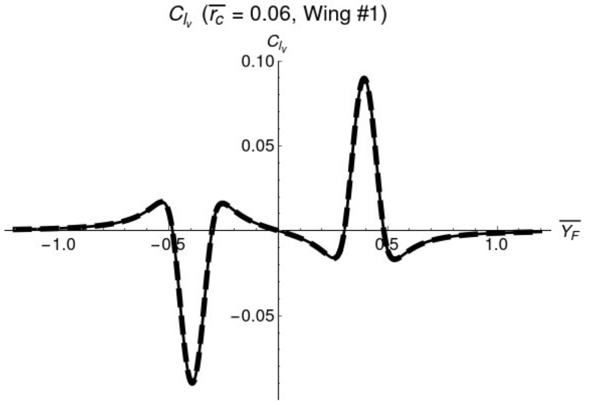

Figure 2.2: Comparison of vortex-induced rolling moment coefficient using analytical method and numerical integration. Dashed line denotes the results obtained using numerical integration and the solid line denotes the analytical solution. Results are shown for the two different wings used in the wind tunnel test.

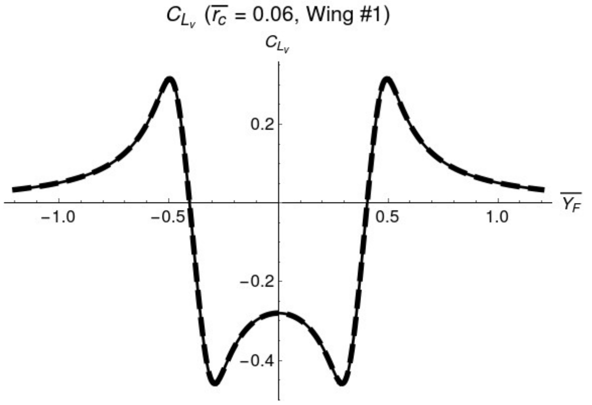

Figure 2.3: Comparison of vortex-induced lift coefficient using analytical method and numerical integration. Dashed line is used for numerical integration and solid line for the analytical solution. Results are shown for the two different wings used in the wind tunnel test.

Summary

A computationally efficient analytical solution for the modified Bowles-Tatnall method has been derived. The computational efficiency of the method will be valuable in performing wake turbulence risk mitigation and safety analyses of newly proposed air traffic management concepts and procedures. These analyses require a significant amount of computations based on large generator-follower matrices of aircraft. It can be also used on the flight deck for advanced future operations such as dynamic self-separation of aircraft.

Acknowledgment

Many thanks to Dr. Roland Bowles for useful discussions on the topic and for reviewing the initial draft of this document. The analytical solutions of vortex-induced lift and rolling moment coefficients were derived with the aid of Mathematica®. We would also like to acknowledge Han Abdali for formatting the equations in MathType®.

References

Ahmad, N.N., VanValkenburg, R.L., Pruis, M.J., Limon Duparcmeur, F., “NASA AVOSS Fast-Time Models for Aircraft Wake Prediction: User’s Guide (APA3.8 and TDP2.1),” National Aeronautics and Space Administration, 2016, NASA/TM–2016–219353.

Bowles, D.R., Personal commmunication. 2014.

Chow, J., Zilliac, G., Bradshaw, P., “Turbulence Measurements in the Near Field of a Wingtip Vortex,” National Aeronautics and Space Administration, 1997, NASA/TM–1997–110418.

Gloudemans, T., Van Lochem, S., Ras, E., Malissa, J.D., Ahmad, N.N., Lewis, T.A., “A Coupled Probabilistic Wake Vortex and Aircraft Response Prediction Model,” National Aeronautics and Space Administration, NASA/TM–2016–219193.

Hinton, D.A., Tatnall, C.R., “A Candidate Wake Vortex Strength Definition for Application to the NASA Aircraft Vortex Spacing System (AVOSS),” National Aeronautics and Space Administration, NASA/TM–1997–110343.

Proctor, F.H., “The NASA-Langley Wake Vortex Modelling Effort in Support of an Operational Aircraft Spacing System”, AIAA Paper 1998-0589.

Proctor, F.H., Hamilton, D.W., Switzer, G.F., “TASS Driven Algorithms for Wake Prediction,” AIAA Paper 2006–1073.

Pruis, M.J., Delisi, D.P., Jacob, D., Lai, D., “Summary of NASA Wake and Weather Data Collection at Memphis International Airport: 2013–2015,” AIAA Paper 2016–3274.

Rich, A., Scheibe, P., Abbasi, N.M., “Rule-based integration: An extensive system of symbolic integration rules,” *The Journal of Open Source Software*, Vol. 3, 2018, pp. 1–3.

Rossow, V., “Validation of Vortex-Lattice Method for loads on wings in lift-generated wakes,” AIAA Paper 1994–1839.

Tatnall, C.R., “A Proposed Methodology for Determining Wake-Vortex Imposed Aircraft Separation Constraints,” MS Thesis, 1995, George Washington University.

Van der Geest, P., “Wake vortex severity criteria: The search for a single metric,” NLR Air Transport Safety Institute, 2012.

Vicroy, D.D., Vijgen, P.M., Reimer, H.M., Gallegos, J.L., Spalart, P.R., “Recent NASA Wake-Vortex Flight Tests, Flow Physics Database and Wake-Development Analysis,” AIAA Paper 1998–5592.

REPORT DOCUMENTATION PAGE

Form Approved
OMB No. 0704-0188

1. REPORT DATE *(DD-MM-YYYY)*
1-06-2019

2. REPORT TYPE
Technical Memorandum

3. DATES COVERED *(From - To)*

4. TITLE AND SUBTITLE
Bowles-Tatnall Wake Vortex Encounter Hazard Metric

5a. CONTRACT NUMBER

5b. GRANT NUMBER

5c. PROGRAM ELEMENT NUMBER

6. AUTHOR(S)
Malissa, Joel; Ahmad, Nashat N.

5d. PROJECT NUMBER

5e. TASK NUMBER

5f. WORK UNIT NUMBER
109492.02.07.01.05

7. PERFORMING ORGANIZATION NAME(S) AND ADDRESS(ES)
NASA Langley Research Center
Hampton, VA 23681-2199

8. PERFORMING ORGANIZATION REPORT NUMBER
L-21029

9. SPONSORING/MONITORING AGENCY NAME(S) AND ADDRESS(ES)
National Aeronautics and Space Administration
Washington, DC 20546-0001

10. SPONSOR/MONITOR'S ACRONYM(S)
NASA

11. SPONSOR/MONITOR'S REPORT NUMBER(S)
NASA-TM-2019-220285

12. DISTRIBUTION/AVAILABILITY STATEMENT
Unclassified-
Subject Category 02
Availability: NASA STI Program (757) 864-9658

13. SUPPLEMENTARY NOTES

14. ABSTRACT Wake vortex spacing standards constrict the terminal area throughput and impose severe constraints on the overall capacity and efficiency of the National Airspace System. For more than two decades starting in the early 1990s, the National Aeronautics and Space Administration conducted extensive research on characterizing the formation and evolution of aircraft wakes. This multidisciplinary work included comprehensive field experiments (Pruis et al. 2016), flight tests (Vicroy et al. 1998), and wind tunnel tests (Rossow 1994; Chow et al. 1997). Parametric studies using large eddy simulations (Proctor 1998; Proctor et al. 2006) were conducted in order to develop fast-time models for the prediction of wake transport and decay (Ahmad et al. 2016). Substantial effort was spent on the formulation of acceptable vortex hazard metrics (Tatnall 1995; Hinton and Tatnall 1997). Several wake encounter severity metrics have been suggested in the past, which include the wake circulation strength, vortex-induced rolling moment coefficient (Clv), bank angle, and the roll control ratio (Tatnall 1995; Hinton and Tatnall 1997; Van der Geest 2012). The vortex-induced rolling moment coefficient introduced by Bowles and Tatnall (Tatnall 1995; Gloudemans et al. 2016) has been used extensively for risk and safety analysis of newly proposed air traffic management concepts and procedures. The original method of Bowles and Tatnall assumed a constant wing loading (the wing lift-curve slope, CLa is constant), which resulted in an overestimation of the vortex-induced rolling moment coefficient.

15. SUBJECT TERMS
Aircraft Wake Turbulence

16. SECURITY CLASSIFICATION OF: a. REPORT	b. ABSTRACT	c. THIS PAGE	**17. LIMITATION OF ABSTRACT**	**18. NUMBER OF PAGES**
U	U	U	UU	15

19a. NAME OF RESPONSIBLE PERSON
STI Help Desk (email: help@sti.nasa.gov)

19b. TELEPHONE NUMBER *(Include area code)*
(757) 864-9658

Standard Form 298 (Rev. 8/98)
Prescribed by ANSI Std. Z39.18